Available online at www.sciencedirect.com
ScienceDirect
Cement and Concrete Research 37 (2007) 221–230
Cement and Concrete Research

Air-void characterisation of foam concrete

E.K. Kunhanandan Nambiar [a], K. Ramamurthy [b,*]

[a] NSS College of Engineering, Palakkad, India
[b] Department of Civil Engineering, Indian Institute of Technology Madras, Chennai-600 036, India

Received 6 February 2006; accepted 24 October 2006

Abstract

The pore structure of cementitious material, predetermined by its porosity, permeability and pore size distribution, is a very important characteristic as it influence the properties of the material such as strength and durability. The pore parameter could therefore be a primary factor influencing the material properties of foam concrete and an in depth look into this aspect is required to establish relationships between this and material properties. In order to evaluate these relationships it was necessary to develop parameters to explain and quantify the air-void structure of foam concrete. This paper discusses the investigations done to characterise the air-void structure of foam concrete by identifying few parameters and influence of these parameters on density and strength. A camera connected to an optical microscope and computer with image analysis software were used to develop these parameters. It is found that out of the air-void parameters investigated, volume, size and spacing of air voids have influence on strength and density. Mixes with a narrower air-void size distribution showed higher strength. At higher foam volume merging of bubbles seems to produce larger voids, results in wide distribution of void sizes and lower strength. Air-void shape has no influence on the properties of foam concrete.

Keywords: Foam concrete; Air void; Image processing; Shape factor; Fly ash replacement

1. Introduction

Foam concrete is a lightweight material consisting of Portland cement paste or cement filler matrix (mortar) with a homogeneous void or pore structure created by introducing air in the form of small bubbles. Introduction of pore is achieved through mechanical means either by preformed foaming (foaming agent mixed with a part of mixing water and aerated to form foam before being added to the mix) and mix foaming (foaming agent mixed with the matrix). The foam concrete discussed in this paper has been manufactured using performed foaming method.

The pore system in cement-based material is conventionally classified as gel pores, capillary pores, macropores due to deliberately entrained air, and macropores due to inadequate compaction. The gel pores do not influence the strength of concrete through its porosity, although these pores are directly related to creep and shrinkage. Capillary pores and other large pores are responsible for reduction in strength and elasticity etc. [1–3]. The above type of pores can be measured by the test methods viz., nitrogen gas absorption–desorption, mercury porosimetry, optical microscopy with image processing and X-ray computed tomography with image processing respectively [4]. The pore systems of autoclaved aerated concrete is classified as (i) artificial air pores, intercluster and interparticle pores [5] (ii) macropores formed due to the expansion of the mass caused by aeration and micropores which appear in the walls between the macropores [6] and (iii) micro capillaries (<50 nm and macro capillaries (>50 nm to 50 μm) and artificial air pores (>50 μm) [7]. In a similar fashion, the pore structure of foam concrete consists of gel pores, capillary pores as well as air voids (air entrained and entrapped pores) [8]. As foam concrete is a self-flowing and self-compacting concrete and without coarse aggregate the possibility of entrapped air is negligible. Empirical models have been proposed to relate porosity and strength of porous solids [9–11]. Based on these models and extending it, a few strength–porosity models have been developed for aerated concrete by Narayanan and Ramamurthy [12]

* Corresponding author. Tel.: +91 44 22574265; fax: +91 44 22574252.
E-mail address: vivek@iitm.ac.in (K. Ramamurthy).

0008-8846/$ - see front matter © 2006 Elsevier Ltd. All rights reserved.
doi:10.1016/j.cemconres.2006.10.009

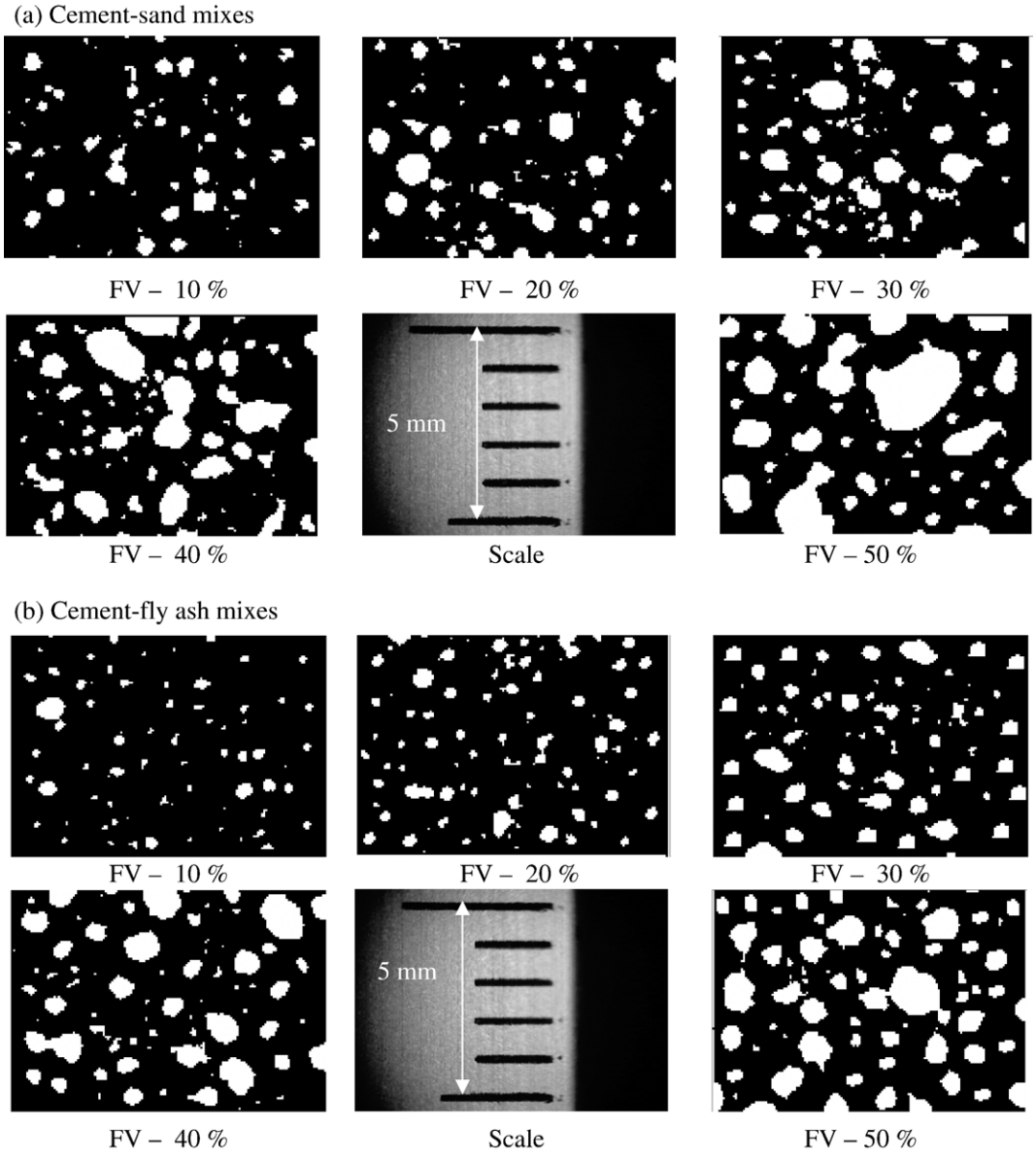

Fig. 1. Typical binary images.

and for foam concrete by Hoff [13] and Kearsley and Wainwright [14]. These models reflect the effect of porosity on the strength and may not adequately represent the pore structure.

According to Cebeci [15], air entraining agents introduce large air voids and do not alter the characteristics of fine pore structure of hardened cement paste appreciably. Kearsley and Visagie [16] reported that the air-void size distribution is one of the most important micro-properties influencing the strength of foam concrete.

The above discussion indicates that the pore parameters could be a primary factor influencing the material properties of foam concrete. Hence an in depth study is necessary to characterise the air voids through certain parameters to explain and quantify the air-void structure of foam concrete. This paper discusses the investigations on air-void structure of foam concrete by identifying few parameters like, volume, size distribution, shape and spacing and influence of these parameters on density and strength. For characterisation of pores of cement-based materials through microscopical studies, image analysis

Table 1
Variation of percentage volume of air voids with foam volume

Foam volume in the mix (%)	Percentage volume of air voids in cement–sand mix based on		Percentage volume of air voids cement–fly ash mix based on	
	Measured fresh density of foam concrete	Image analysis of hardened foam concrete	Measured fresh density of foam concrete	Image analysis of hardened foam concrete
10	8.93	11	9.23	10.43
20	18.76	18.66	19.01	18.81
30	28.90	27.79	28.61	28.13
40	37.90	36.70	38.01	36.41
50	47.34	44.44	47.94	44.84

has been successfully used [8,17–20]. In this study, air-void parameters of foam concrete were measured using an image analysis software on images of prepared surfaces of specimens captured by an optical microscope.

2. Experimental investigations

2.1. Constituent materials

The constituent materials used to produce foamed concrete comprised of (i) ordinary Portland cement conforming to IS 12269–1897 [21], (ii) pulverized river sand finer than 300 microns (specific gravity = 2.52), (iii) class F fly ash (specific gravity = 2.09) conforming to ASTM C 618–1989 [22], and (iv) foam produced by aerating an organic based foaming agent (dilution ratio 1:5 by weight) using an indigenously fabricated foam generator to a density of 40 kg/m^3. The water–solids ratio of these mixes were arrived based on (i) the stability of the foam concrete mix which is defined as the state of condition at which measured density is equal to or nearly equal to design density and (ii) the consistence of mix (for a flow cone spread value of 45 ± 5%) [23].

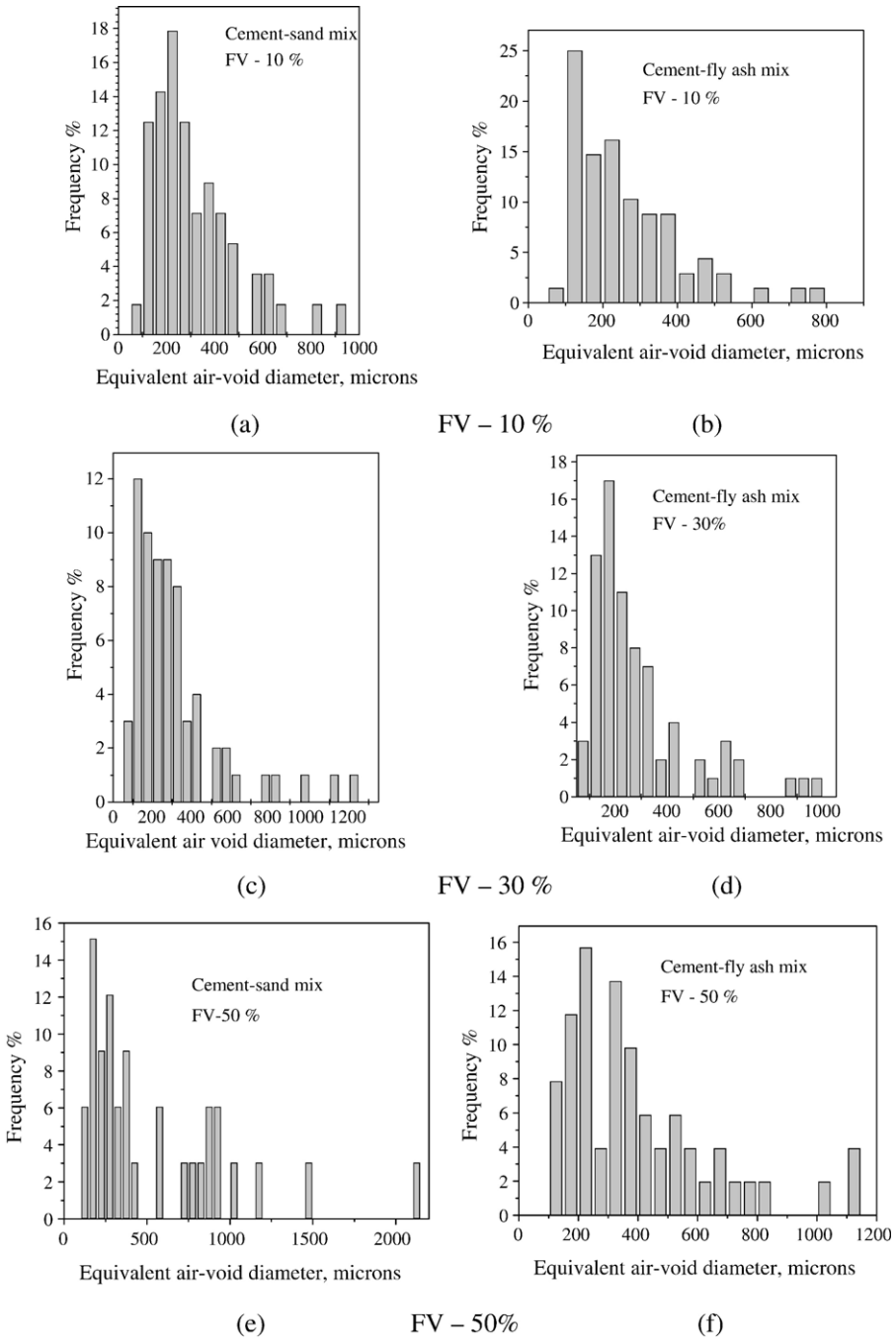

Fig. 2. Air-void size distribution for cement–sand (a,c,e) and cement–fly ash mixes (b,d,f).

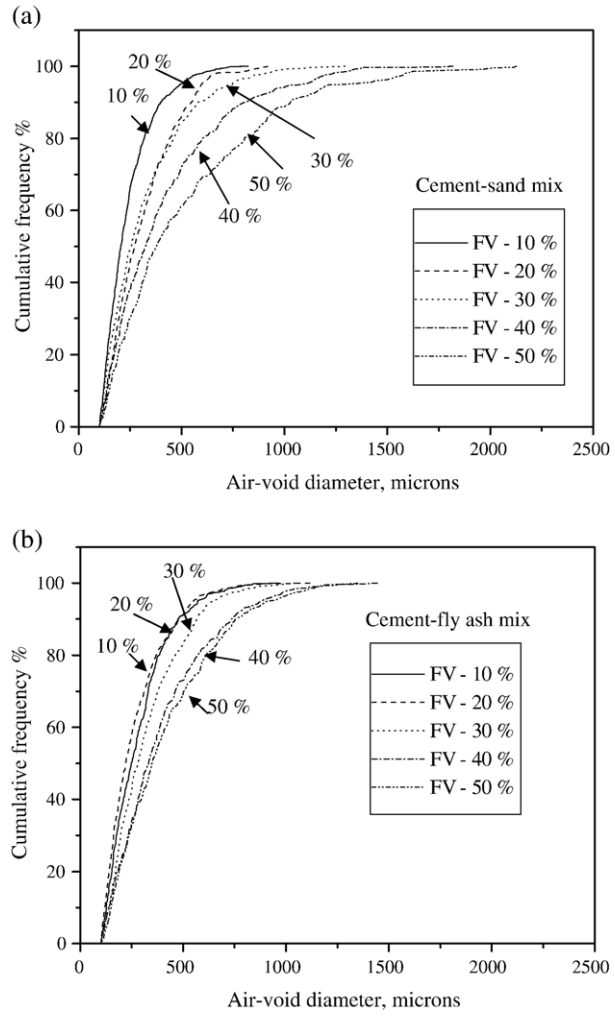

Fig. 3. Cumulative frequency distribution of air-void sizes (average): (a) cement–sand mix and (b) cement–fly ash mix.

2.2. Specimen and surface preparation

Foam concrete mixes used for the study include cement–sand and cement–fly ash mixes (FA-100%) with a filler–cement ratio of 2 and varying foam volume (10% to 50%). For each mix, 4 cube specimens of size 50 mm were cast and moist cured till testing. The cubes were then cut into slices of 25 mm thick, parallel and perpendicular to the cast face and at different depths of specimen, in order to get 6 pieces of specimen (cut surfaces) from each sample using a diamond rotary saw. The dimensions of specimen for image analysis were 50 × 50 × 25 mm. These 6 surfaces for each foam concrete mix were first analysed to verify the uniformity in distribution of air voids, when cut from different directions. An important requirement for successful application of image analysis is a sufficient contrast between pores and matrix. The quality of the surface treatment is important because any surface defect can be mistaken for an air void and can thus become a significant source of error. The conventional surface preparation method of filling pores with synthetic resin and smoothening by grinding is not suitable for foam concrete because new pore gets opened during grinding and polishing operations, which have to be filled with resins again [20]. Hence the specimens were first carefully polished in a machine to attain a surface on which the boundaries of the air voids and matrix are sharp and easily distinguishable. The specimens were cleaned with compressed air and placed in the oven at 50 °C to get a dry surface. This surface was applied 2 coats of black ink using a permanent marker pen and allowed to dry. White talc powder was then spread on the polished surface, and slowly worked into the air voids with a flat face of a glass slide. The excess powder was wiped away with the edge of a razor blade and then with a lightly oiled finger tip, leaving only the powder that had been worked into the air voids. Only foam concrete specimens with excellent quality surface are subjected to image analysis measurement.

2.3. Image processing and analysis

Image analysis system consisted of an optical microscope and a computer with image analysis software. As the objective is to investigate the structure of the macropores of foam concrete which is considered as pores having diameter larger than 50 μm [7], a magnification of 20× was selected with a pixel representing 16 microns and each image covering 44.23 mm^2 (7.68 mm × 4.23 mm). A total of 30 images were captured for each mix all together from the six cut surface. Each image is digitized, converted into binary form and a few morphological operations were done to refine the form of objects. Five such operations found to be useful in application to concrete microscopic images are dilation, erosion, opening, closing, and hole fill. Between auto-threshold and hole-fill functions, many scenarios can be proposed to achieve the goal of enhancing the features of interest [24]. Different combinations of the above operations were tried and the number of iterations of such operations required depended on the quality of the image. Simple operations were only needed for this study as the air voids of white colour contrast sharply with the surrounding matrix of black colour, producing almost similar to a binary image prior to the microscopic examination. Typical binary images for two mixes (cement–sand and cement–fly ash) are shown in Fig. 1 (a) and (b).

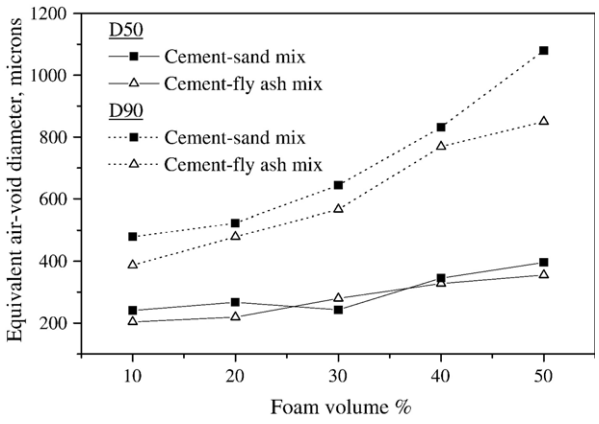

Fig. 4. Variation of D 50 and D 90 with foam volume.

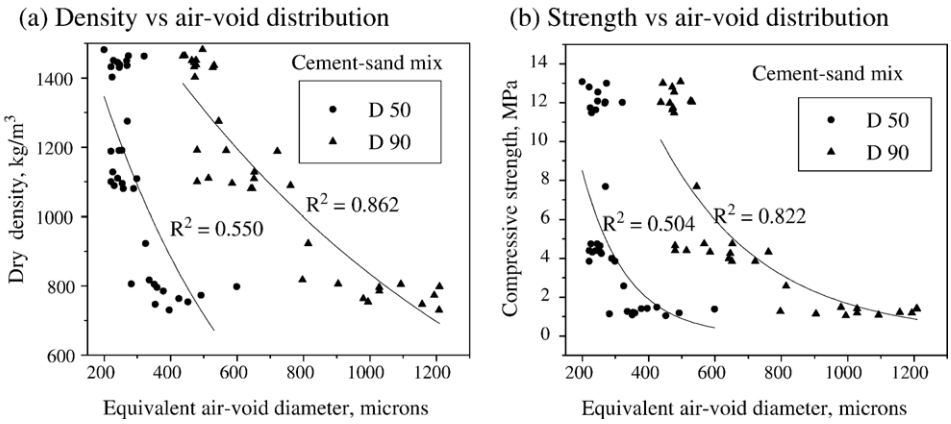

Fig. 5. Density and strength vs. air-void size distribution parameters (cement–sand mix).

After completing the image processing and air-void identification, the total area, perimeter, equivalent diameter of every defined area (air void) in the image was stored in Excel format and analysed for obtaining the parameters for the air voids such as percentage of voids, air-void size distribution, shape of the pores in terms of shape factor and spacing factor for each mixes.

3. Characterisation of air voids

3.1. Volume of air voids

Table 1 shows the variation of percentage volume of air voids with the volume of foam added computed from fresh density measurements and through image analysis in foam concrete with cement–sand and cement–fly ash mixes.

As the water–solids ratio for each mix is chosen to achieve a stable mix, i.e. to provide a density ratio of 1 (design density to obtained density), the difference between foam volume added and the measured fresh density of foam concrete is almost closer.

In mixes with 20% and higher foam volume, the percentage volume voids measured in hardened foam concrete is marginally lower as compared to volume of voids calculated based on measured fresh density. This difference may be attributed to error in interpretation likely to occur i) as all the voids are not cut exactly through its centre while cutting the specimen, results in sizes distribution smaller than that of actual air-void sizes ii) when air voids overlap each other, as can be seen from Fig. 1, and (iii) when the air void touches the boundaries of the image. As the foam volume increases the reduction in measured value increases. Most of the specimen exhibited marginally higher density than the designed density and to some extent the lowering of this value can be explained by this.

In mix with 10% foam volume, the percentage volume of voids estimated through image analysis was higher than the foam volume added. This overestimation may be due to difficulty in discriminating air voids from surface defect or other artifacts such as sticking of the talc powder used for pore filling. This possibility is more at low foam volume as the majority of the pores are of uniform and smaller size (as can be seen later) and as most such defects unfortunately fall in the same narrow size range.

3.2. Air-void size distribution parameters

The frequency distribution of air-void sizes in Fig. 2 shows that the majority of the voids are of uniform size. There are a few bigger sized pores present and their number also increases

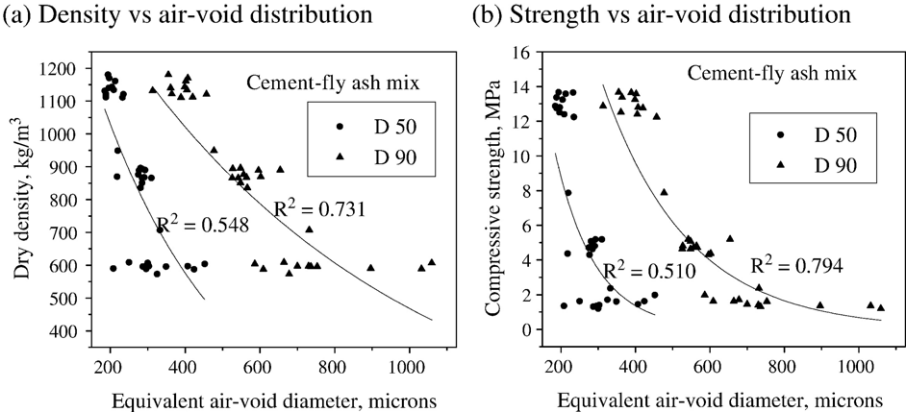

Fig. 6. Density and strength vs. air-void size distribution parameters (cement–fly ash mix).

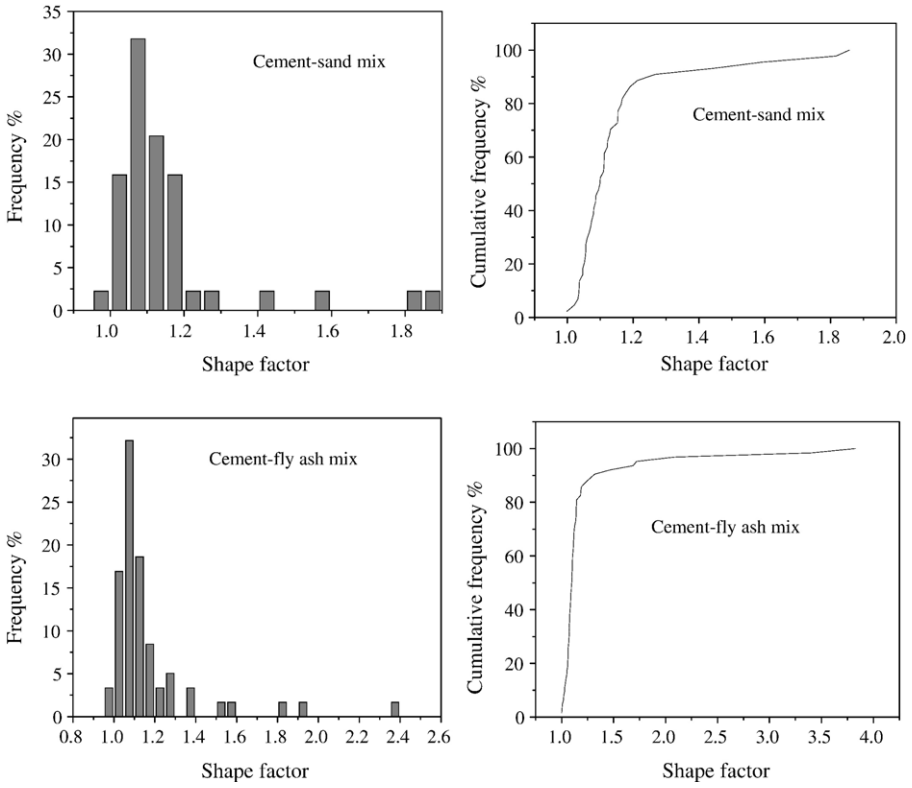

Fig. 7. Frequency histogram and cumulative frequency % curve (FV — 30%).

with an increase in foam volume, which may be due to the possibility of merging and overlapping of pores at higher foam content [25]. Referring to cumulative frequency distribution in Fig. 3, at low dosage of foam volume the air-void distribution is more uniform than at high foam volume content. This uniformity is relatively predominant in foam concrete with cement–fly ash mixes as compared to cement–sand mixes. In order to quantify and compare the air-void size distribution of different mixes and to evaluate its influence on the strength and density of foam concrete, the parameters used are D 50 and D 90 (10% oversize).

These two parameters can be read from Fig. 3 (a) and (b) and the variation with foam volume is shown in Fig. 4 for both the mixes. The median air-void size varies between 200 and 400 microns. In a study of the bubble size distribution of the foam, it was observed that the bubble size varied mostly between 200 and 450 microns with a median value at 350 microns. Both D 50 and D 90 increase with foam volume, but the size of larger voids increases sharply with foam volume. These parameters are smaller for cement–fly ash mix, suggesting that the inclusion of fly ash helps in achieving more uniform distribution of air voids than fine sand. Similar observations were made through a study on fineness of sand on compressive strength of foam concrete [26]. As the filler becomes finer, a more uniform distribution of air voids is achieved probably by providing a uniform coating of the paste on each bubble thereby preventing it from merging and overlapping.

Figs. 5 and 6 represent density and strength as a function of the air-void size parameters for foam concrete with cement–sand and cement–fly ash mixes. As the density increased the median void diameters become smaller (Figs. 5(a) and 6(a)). At higher densities, D 90 (10% oversized voids) also become smaller. It is also to be noted that the D 50 and D 90 curves converge at higher densities (with low foam volumes) indicating that voids become smaller and more uniform in size in this range.

An increase in median diameter of air voids leads to reduction in strength (Figs. 5 (b) and 6(b)). But at higher densities the air-void distribution does not seem to have an influence on compressive strength, which may be because of attaining more uniform distribution of voids at low foam volume ranges or

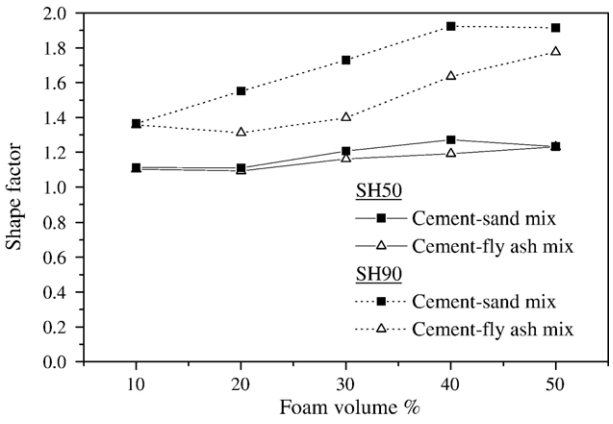

Fig. 8. Variation of SH 50 and SH 90 with foam volume.

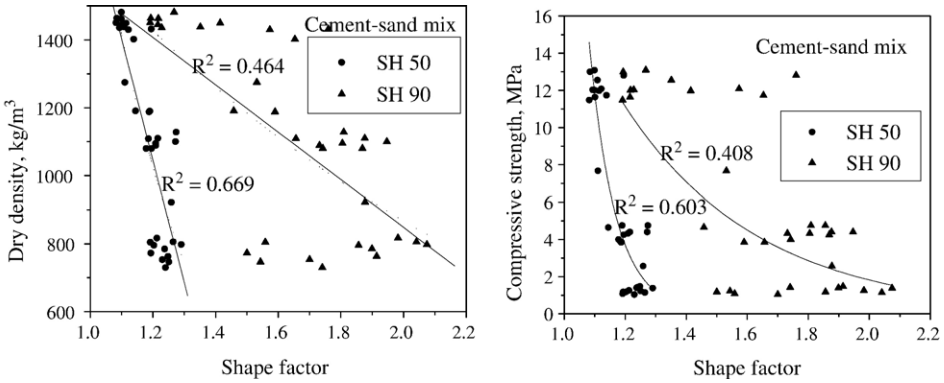

Fig. 9. Density and strength vs. shape factor parameters (cement–sand mix).

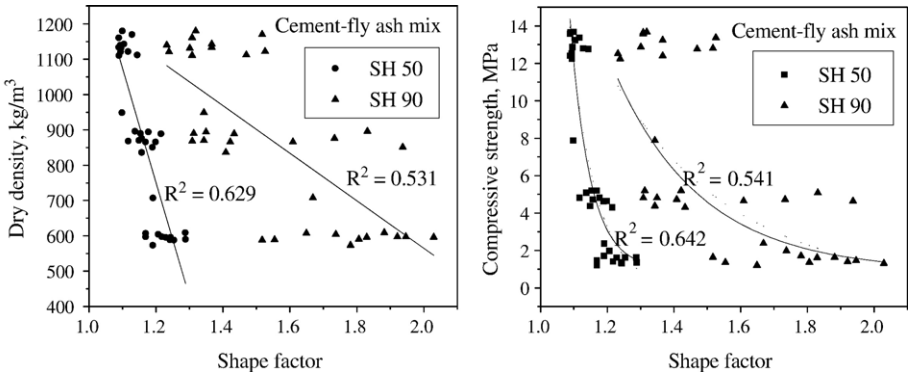

Fig. 10. Density and strength vs. shape factor parameters (cement–fly ash mix).

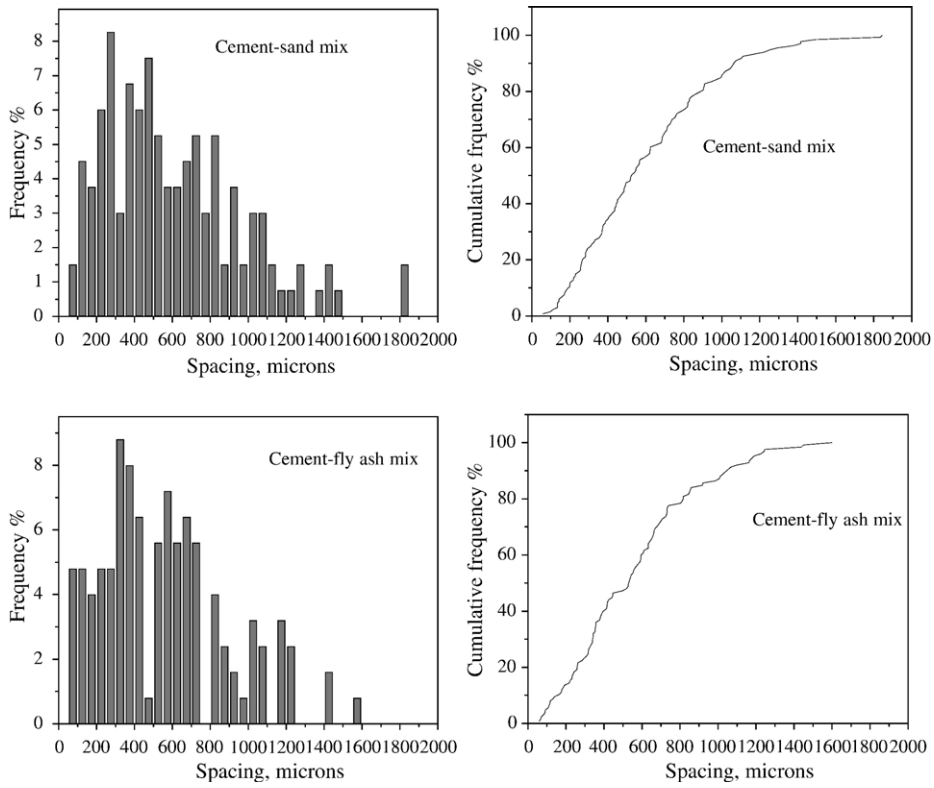

Fig. 11. Frequency histogram and cumulative frequency curve for spacing (FV — 30%).

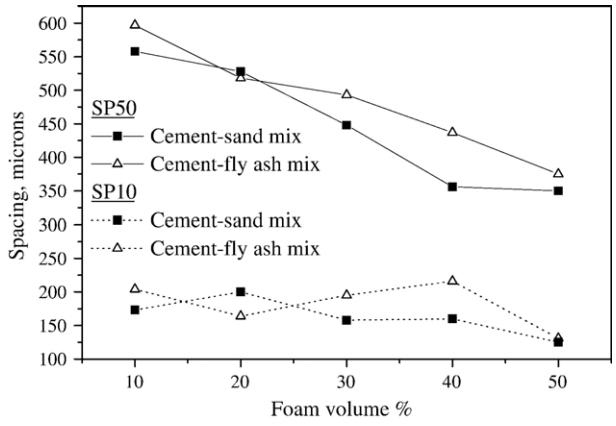

Fig. 12. Variation of SP 50 and SP 10 with foam volume.

higher density ranges. Similar observation was reported by Visagie and Kearsley [8]. D 90 correlates better than D 50 with strength for both the mixes, showing that compared to smaller pores it is the bigger pores that influence the strength of foam concrete. This corroborates with the observations of Luping [10] that the materials having the same matrix and porosity, the strength of the material containing more large-size pores are lower. Compared to cement–sand mixes, the correlation between D 90 and strength is lower in cement–fly ash mixes, indicating that the effect of air-void size parameter is more predominant in cement–sand mixes.

3.3. Air-void shape parameter

The shape factor defines the geometry of the voids and is a function of outer perimeter and surface area for each void obtained through image analysis and is given by

$$\text{Shape factor (SH)} = \frac{(\text{Perimeter})^2}{4\pi(\text{Area})}$$

Shape factor equals unity for a perfect circle and is larger for irregular shaped voids. Similar concepts have been used by Lange et al. [18] and Zhang et al. [27]. A typical shape factor frequency histogram and cumulative frequency distribution curve are shown in Fig. 7 for foam concrete with cement–sand and cement–fly ash mixes. From the cumulative frequency diagram it is evident that shape of the voids is similar and only negligible number of voids is having irregularity. Compared to foam concrete with sand as filler, mixes with fly ash exhibit more uniform shape. This is attributed to the uniform distribution of bubbles without merging and overlapping in a mix containing finer materials like fly ash.

The influence of foam volume on the shape factor for both the mixes is shown in Fig. 8. SH 50 represents the median value of observed shape factors of pores. Shape factor at SH 90 represents that 90% of the observed shape factor values are lower than (or 10% of the values are higher than) this value, showing the extreme values of shape factor or irregularity of pores. The median shape factor (SH 50) remains almost constant (1.1 to 1.23), which indicates that practically most of the air voids are nearly spherical unlike aerated concrete where the expansion of concrete during gas formation results in the development of ellipsoidal oriented pores [28]. However a few higher values of shape factor (1.6 to 1.8) represent irregular pores produced due to merging of bubbles at higher foam volume (Fig. 2). Figs. 9 and 10 show the correlation between shape factor and density and strength of foam concrete with cement–sand and cement–fly ash mixes. It can be seen that there is no correlation between strength and density with shape factor. This is due to the fact that all air voids are of approximately same shape and independent of foam volume.

3.4. Air-void spacing factor

The smallest distance through the matrix between two voids in the vicinity is measured as spacing of air voids on the images using the manual measurement options given in the analysis software. The frequency histogram and cumulative distribution curves for typical cement–sand and cement–fly ash mixes are given in Fig. 11. Similar to other air-void parameters, spacing parameters are represented by SP 50 and SP 10, obtained from the cumulative distribution curve. SP 10 represents that spacing of which 10% are below this value. In the case of spacing, it is the minimum spacing which is going to be the critical for

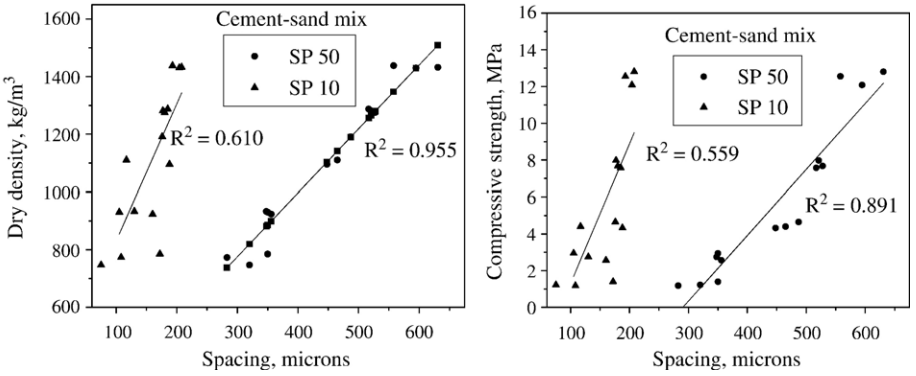

Fig. 13. Density and strength vs. spacing factor parameters (cement–sand mix).

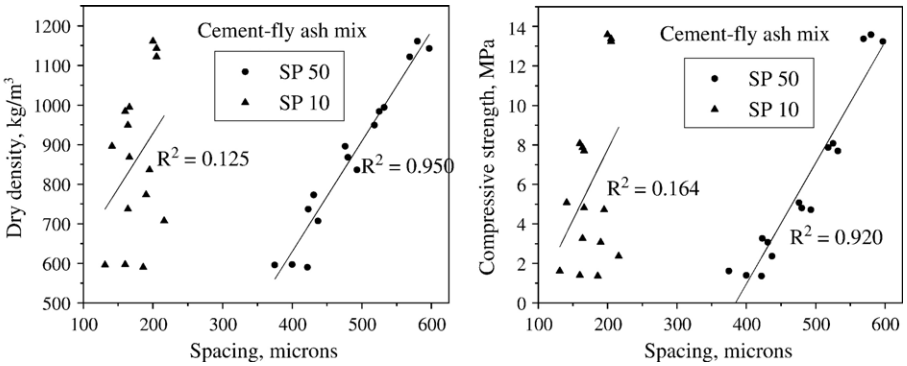

Fig. 14. Density and strength vs. spacing factor parameters (cement–fly ash mix).

strength and therefore 10% value is taken as the parameter different from that of diameter (90% value) where maximum diameter is the critical value.

The variations of spacing factor with foam volume for both the mixes are shown in Fig. 12. An increase in foam volume causes reduction in SP 50, while SP 10 exhibit marginal variation. This reduction in spacing is attributed to reduction in paste phase with an increase in foam volume. The relationship between these spacing factors and strength and density are shown in Figs. 13 and 14 for cement–sand and cement–fly ash mixes respectively. In general, as spacing increases the strength and density increase. Only mean spacing factor (SP 50) correlates highly with the strength and density. Even though SP 10 showed a very poor correlation with strength, a closer look into the data reveals that disregarding lower density range where there is high scattering, correlation exists for other densities, i.e. at higher density it may have an effect on strength.

4. Conclusions

Considering as a primary factor influencing strength and density, the air voids in foam concrete are characterised and air-void parameters are developed. The air voids are characterised on the basis of volume, size distribution, shape and spacing and based on this following conclusions are made:

- Out of the air-void parameters investigated, volume, size and spacing have influence on strength and density.
- Inclusion of fly ash as a filler in foam concrete helps in achieving more uniform distribution of air voids than fine sand. Fly ash being finer, helps in uniform distribution of air voids by providing a well and uniform coating on each bubbles and preventing it from merging and overlapping.
- D 90 correlates better than D 50 with strength for both the mixes, showing that compared to smaller pores it is the bigger pores that influence the strength of foam concrete.
- Mixes with a narrower air-void size distribution showed higher strength. At higher foam volume merging of bubbles seems to produce larger voids, results in wide distribution of void sizes and lower strength.
- Air-void shape has no influence on the properties of foam concrete as all air voids are of approximately same shape and independent of foam volume.
- A clear relationship between SP 50 with strength and density are observed, in general as spacing increases the strength and density increase. There is no clear correlation between SP 10 with strength and density, but at higher density it may have an effect on strength.

References

[1] P.K. Mehta, P.J.M. Monteiro, Concrete: Microstructure, Properties, and Materials, Indian Concrete Institute, 1997.
[2] A.M. Neville, J.J. Brooks, Concrete Technology, Pearson Education Pvt. Ltd., Singapore, 2004.
[3] R. Kumar, B. Battacharjee, Porosity, pore size distribution and in situ strength of concrete, Cement and Concrete Research 33 (2003) 155–164.
[4] H. Uchikawa, S. Uchida, S. Hanehara, Measuring method of pore structure in hardened cement paste, mortar and concrete, II Cemento 2 (1991) 67–90.
[5] P. Prim, F.H. Wittmann, Structure and water absorption of aerated concrete, in: F.H. Wittmann (Ed.), Autoclaved Aerated Concrete, Moisture and Properties, Elsevier, Amsterdam, 1983, pp. 43–53.
[6] J. Alexanderson, Relation between structure and mechanical properties of autoclaved aerated concrete, Cement and Concrete Research 9 (1979) 507–514.
[7] S. Tada, S. Nakano, Microstructural approaches to properties of mist cellular concrete, in: F.H. Wittmann (Ed.), Autoclaved Aerated Concrete, Moisture and Properties, Elsevier, Amsterdam, 1983, pp. 71–88.
[8] M. Visagie, E.P. Kearsely, Properties of foamed concrete as influenced by air-void parameters, Concrete Beton 101 (2002) 8–14.
[9] M. Roßler, I. Odler, Investigations on the relationship between porosity, structure and strength of hydrated Portland cement pastes, Cement and Concrete Research 15 (2) (1985) 320–330.
[10] T. Luping, A study of the quantitative relationship between strength and pore-size distribution of porous materials, Cement and Concrete Research 16 (1986) 87–96.
[11] K.L. Watson, Autoclaved aerated concrete from slate waste part 2: some property/porosity relationship, International Journal of Lightweight Concrete 2 (3) (1980) 121–123.
[12] N. Narayanan, K. Ramamurthy, Prediction relations based on gel-pore parameters for the compressive strength of aerated concrete, Concrete Science and Engineering 1 (2) (2000) 206–212.
[13] G.C. Hoff, Porosity–strength considerations for cellular concrete, Cement and Concrete Research 2 (1972) 91–100.
[14] E.P. Kearsley, P.J. Wainwright, The effect of porosity on the strength of foamed concrete, Cement and Concrete Research 32 (2002) 233–239.
[15] O.Z. Cebeci, Pore structure of air-entrained hardened cement paste, Cement and Concrete Research 11 (1981) 257–265.
[16] E.P. Kearsely, M. Visagie, Micro-properties of foamed concrete, in: R.K. Dhir, N.A. Handerson (Eds.), Specialist Techniques and Materials for Construction, Thomas Telford, London, 1999, pp. 173–184.
[17] S. Chatterji, H. Gudmundsson, Characterization of entrained air bubble systems in concretes by means of an image analyzing microscope, Cement and Concrete Research 7 (1977) 423–428.

[18] D.A. Lange, H.M. Jennings, S.P. Shah, Image analysis techniques for characterisation of pore structure of cement-based materials, Cement and Concrete Research 24 (5) (1994) 841–853.
[19] R. Pleau, M. Pegeon, J.L. Laurencot, Some findings on the usefulness of image analysis for determining the characteristics of the air void system on hardened concrete, Cement and Concrete Composites 23 (2001) 237–246.
[20] E. Petrov, Schlegel, Application of automatic image analysis for the investigation of autoclaved aerated concrete structure, Cement and Concrete Research 24 (1994) 830–840.
[21] IS 12269, Specifications for 53 Grade Ordinary Portland Cement, Bureau of Indian Standards, New Delhi, 1987.
[22] ASTM C 618, Standard specification for fly ash and raw or calcined natural pozzolana for use as a mineral admixture in Portland cement concrete, Annual Book of ASTM Standards, vol. 04.02, American Society of Testing and Materials, Philadelphia, 2002.
[23] E.K.K. Nambiar, K. Ramamurthy, Models relating mixture composition to the density and strength of foam concrete using Response Surface Methodology, Cement and Concrete Composites 28 (9) (2006) 752–760.
[24] P. Soroushian, M. Elzafraney, Morphological operations, planar mathematical formulations, and stereological interpretations for automated image analysis of concrete microstructure, Cement and Concrete Composites 27 (2005) 823–833.
[25] R. Pleau, P. Plante, R. Gagne, M. Pigeon, Practical considerations pertaining to the microscopical determination of air-void characteristics of hardened concrete (ASTM C 457 standard), Cement, Concrete and Aggregates 12 (2) (1990) 3–11.
[26] E.KK. Nambiar, K. Ramamurthy, Influence of filler type on the properties of foam concrete, Cement and Concrete Composites 28 (5) (2006) 475–480.
[27] Z. Zhang, F. Ansari, N. Vitillo, Automated determination of entrained air-void parameters in hardened concrete, ACI Materials Journal 102 (1) (2005) 42–48.
[28] R. Cabrillac, B. Fiorio, A. Beaucour, H. Dumontet, S. Ortola, Experimental study of the mechanical anisotropy of aerated concrete and of the adjustment parameters on the induced porosity, Construction and Building Materials 20 (2006) 286–295.